

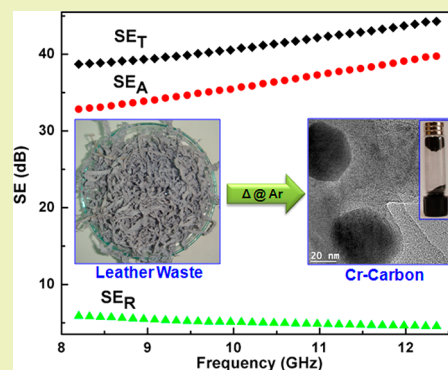
Conversion of Industrial Bio-Waste into Useful Nanomaterials

Meiyazhagan Ashokkumar,[†] Narayanan Tharangattu Narayanan,[‡] Bipin Kumar Gupta,[§] Arava Leela Mohana Reddy,[‡] Avanish Pratap Singh,[§] S. K. Dhawan,[§] Bangaru Chandrasekaran,[†] Dinesh Rawat,^{||} Saikat Talapatra,^{||} Pulickel M. Ajayan,[‡] and Palanisamy Thanikaivelan^{*,†,‡}[†]Advanced Materials Laboratory, Centre for Leather Apparel & Accessories Development, Central Leather Research Institute (Council of Scientific and Industrial Research), Adyar, Chennai 600020, India[‡]Department of Mechanical Engineering and Materials Science, Rice University, Houston, Texas 77005, United States[§]National Physical Laboratory (Council of Scientific and Industrial Research), Dr K S Krishnan Road, New Delhi 110012, India^{||}Department of Physics, Southern Illinois University Carbondale, Carbondale, Illinois 62901, United States

S Supporting Information

ABSTRACT: Chromium-complexed collagen is generated as waste during processing of skin into leather. Here, we report a simple heat treatment process to convert this hazardous industrial waste into core-shell chromium-carbon nanomaterials having a chromium-based nanoparticle core encapsulated by partially graphitized nanocarbon layers that are self-doped with oxygen and nitrogen functionalities. We demonstrate that these core-shell nanomaterials can be potentially utilized in electromagnetic interference (EMI) shielding application or as a catalyst in aza-Michael addition reaction. The results show the ability to convert industrial bio-waste into useful nanomaterials, suggesting new scalable and simple approaches to improve environmental sustainability in industrial processes.

KEYWORDS: Cr-carbon, Conductivity, Magnetism, Leather shavings, Catalysis, Shielding



■ INTRODUCTION

Research on carbon materials has become a hot area in recent decades mainly due to its potential applications such as catalyst supports, adsorbents, biologically implantable materials, electrodes, sensors, energy storage media, fuel cells, solar cells, displays, and molecular electronic devices.¹ Fullerene, carbon nanotubes, graphene, and graphite with increasing dimensions are classical examples of carbon materials with excellent mechanical, electronic, optical, and thermal properties.² Nevertheless, inorganic materials have also been extensively studied in the form of nanofibers, nanowires, or nanotubes for a rich variety of applications including tissue engineering, sensing, and energy storage.^{3,4} Hybrid inorganic-organic core-shell nanostructures are being produced to achieve improved property profiles resulting from the integration of distinct features of the individual components.⁵ For example, carbon coated with inorganic nanomaterials such as Si and LiFePO₄ has been prepared for Li-ion battery applications.^{5,6} However, lengthy and stringent process conditions pose significant challenges to the synthesis of core-shell organic-inorganic hybrid materials, and the use of expensive precursors hinders commercial applications. In this context, the availability of a chromium-complexed carbon source, leather, as waste with negligible cost, will be an added advantage in synthesizing transition metal-carbon core-shell materials.

Recently, we have synthesized self-doped carbon nano-onion materials for energy storage applications from pristine collagen waste through a simple high temperature treatment.^{7,8} The global leather industry generates 0.8 million ton of chrome shaving waste every year.⁹ Chrome shavings are small thin pieces of chrome-tanned leather formed during the shaving operation.⁹ It primarily consists of chromium, amounting to about 3% (as Cr₂O₃ on dry weight basis), complexed with side-chain carboxylic groups of collagen molecules. Because of the stringent control on the disposal of chromium-containing waste in many parts of the world as well as the presence of a valuable protein source, the leather industry is looking to utilize these wastes.⁹ Although there are several techniques available to utilize the chromium-containing leather waste, development of advanced multifunctional materials with high value is gaining importance.^{8,9} Herein, we report an efficient procedure for direct conversion of chrome shaving waste into a core-shell chromium-nanocarbon (Cr-carbon) multifunctional material by a simple heat treatment, which has potential for various applications.

Received: December 4, 2012

Revised: April 13, 2013

Published: April 18, 2013

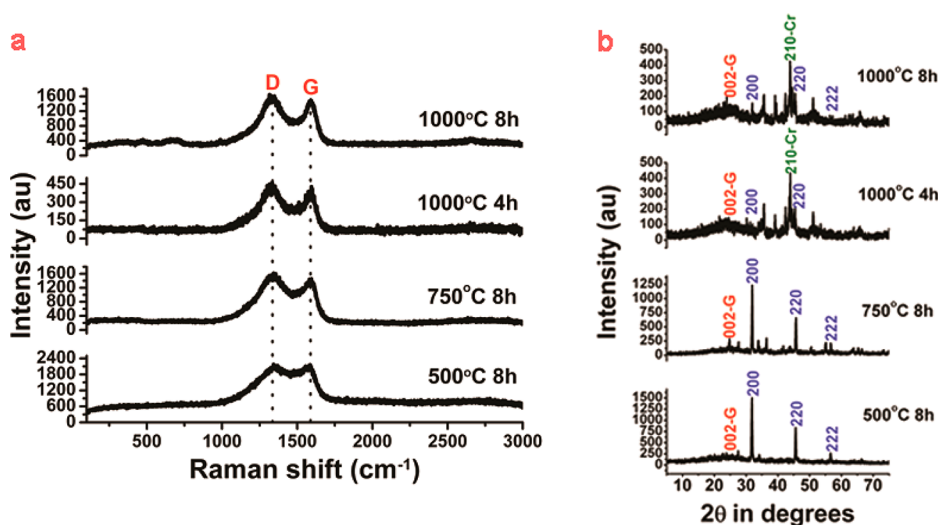


Figure 1. Raman and XRD characterization of the Cr–carbon core–shell materials derived from chrome shaving waste. (a) Raman spectra and (b) X-ray diffraction analysis of select Cr–carbon materials derived from heat treatment of chrome shaving waste at different temperatures and time.

EXPERIMENTAL SECTION

Synthesis of Cr–Carbon Core–Shell Materials from Chrome Shaving Waste. The chrome shaving waste used in this work was collected from the pilot tannery at Central Leather Research Institute, Chennai, India. About 15 g of this waste was transferred to a vertical Inconel reactor without any further treatment and purged with high purity argon gas at a flow rate of 25 mL/min for 10 min. After purging, the reactor was heated at a heating rate of 5 °C/min to the desired temperatures (500, 750, and 1000 °C) and held at that temperature for different durations (4 and 8 h). After the reaction, the temperature was gradually stepped down to room temperature under the same argon atmosphere. The volatile products were removed from the reactor by the continuous flow of argon gas.

Characterization of the Cr–Carbon Core–Shell Materials. The Raman spectra of the Cr–carbon core–shell materials were obtained with a Renishaw InVia laser Raman microscope using a 50× objective lens, 632.8 nm (He–Ne) laser beam, and 1800 lines per mm grating. X-ray diffractograms (XRD) were obtained using a Rigaku diffractometer, operating with CuK α radiation ($\lambda = 0.15406$ nm) generated at a voltage of 30 kV and current of 20 mA at a scan rate of 3° per min. X-ray photoelectron spectroscopy (XPS) analysis was carried out on a PHI Quantera X-ray photoelectron spectrometer with a chamber pressure of 5×10^{-9} Torr and an Al cathode as the X-ray source. The source power was set at 100 W, and pass energies of 140.00 eV for survey scans and 26.00 eV for core-level scans were used. High resolution transmission electron microscopy (HR-TEM) analysis of the Cr–carbon material derived by treating the chrome shaving waste at 1000 °C for 8 h (sonicated in ethanol) was carried out using a JEOL 2100 Field Emission Gun TEM in a holey carbon grid. The electrical conductivity of the formed Cr–carbon core–shell materials was measured after pressing them into a disc of 1.4 mm diameter and 0.5 mm thickness using a two probe 4.5 digit micro-ohm meter (model no. PE-16R, Prestige Electronics, Mumbai, India). Room temperature magnetic measurement on the as-synthesized Cr–carbon sample (1000 °C for 8 h) was measured using a vibrating sample magnetometer (VSM, Lakeshore model 7407). Photo luminescence (PL) characterization of the Cr–carbon sample (1000 °C for 8 h) was carried out using a luminescence spectrometer (Nanolog, HORIBA, Jobin Yvon) with xenon flash lamp as the source of excitation. The elemental analysis of the Cr–carbon materials was carried out using EURO EA elemental analyzer.

Electromagnetic Interference Shielding and Catalysis Applications of the Cr–Carbon Core–Shell Materials. For the EMI shielding application study, the Cr–carbon sample (1000 °C for 8 h) was mixed with nonconducting and diamagnetic polyvinyl chloride (used as a binder) in 1:0.17 ratio and made into a pellet with

22.8 mm \times 10 mm \times 3 mm dimensions. EMI shielding measurements were carried out using Agilent E8362B Vector Network Analyzer in a microwave range of 8.2–12.4 GHz (X-band). For the catalysis study, the Cr–carbon material derived from chrome shaving waste (1000 °C for 8 h) was activated using 10 N nitric acid with continuous stirring for 12 h at 70 °C. The reaction mixture was then cooled to room temperature and washed several times with deionized water. The washings and filtration were repeated until the pH of the washings reached 7. The sample was completely dried in a hot air oven and used as a catalyst in aza-Michael addition reaction of aliphatic amines with α , β -unsaturated compounds. The aza-Michael addition reaction was carried out by using a mixture of aliphatic amine (1 mmol), Michael acceptor (1.2 mmol), and activated Cr–carbon (2.5 mg) as a catalyst. The reaction mixture was stirred at room temperature, and the completion of the reaction was monitored by using a thin layer chromatography (TLC) plate (SiO₂). After completion of the reaction, the reaction mixture was extracted three times using dichloromethane (each 15 mL). The combined organic phase was concentrated under vacuum evaporation, and the resulting crude product was purified using silica column chromatography to obtain the desired product.

RESULTS AND DISCUSSION

Raman and X-ray Diffraction Studies of Cr–Carbon.

Raman spectra of the core–shell nanostructures derived from chrome shavings show characteristic bands at 1332 and 1586 cm^{-1} , as shown in Figure 1a. The former corresponds to a D band showing the presence of defects in the graphitic lattice with A_{1g} symmetry, while the latter peak, namely, a G band, is associated with the in-plane E_{2g} mode of single crystalline graphitic carbon atoms in the honeycomb lattice.¹⁰ Broadening of both the D and G bands decreased as the temperature and heat duration increased, indicating more graphitization with substantial defects. The presence of O and N, as verified later by XPS analysis, may contribute to the increased defects.

The XRD patterns (Figure 1b) reveal the presence of chromium-based nanoparticles along with graphitic carbon in our synthesized core–shell nanomaterials. Indeed, the diffraction peaks, such as (002) and (101) associated with the graphitic carbon, seem to be suppressed by the strong appearance of chromium-based nanoparticles. The phases of chromium oxide (Cr₂O₃; JCPDS PDF# 00-059-0308) nanoparticles along with low-intense graphitization peaks are noted only for the core–shell nanostructures derived from low

temperature treatment of chrome shaving waste (500 and 750 °C). On the other hand, higher temperature treatment (1000 °C) of chrome shaving waste shows a mixed phase with diffraction peaks corresponding to Cr_2O_3 as well as Cr. The major peak identified was indexed as (210), corresponding to Cr (JCPDS PDF# 00-019-0323), and a few other peaks were indexed for Cr_2O_3 (JCPDS PDF# 00-059-0308). The size of Cr-based nanoparticles calculated from Scherrer's equation based on the (210) diffraction peak was found to be ~ 42 nm.¹¹ However, other phases did not match well with either Cr or Cr_2O_3 . Although the nature of these new diffraction peaks is not entirely certain, it seems possible that they are associated with the coordination of Cr to O-based ligands. At high temperature (1000 °C), it is possible that Cr_2O_3 may destabilize and be converted to Cr and may coordinate with available O species.¹² Although the formation of chromium carbides (Cr_3C_2) is possible at a high temperature reductive environment, the phases obtained for our sample does not match with the more stable form of (Cr_3C_2).¹³

X-ray Photoelectron Spectroscopy. XPS is an excellent tool to identify the possible atomic composition and functionalities of as-synthesized core-shell nanostructures. Our core-shell nanostructures synthesized from chrome shaving waste at different temperatures are composed of C, O, N, and Cr in the range of 66.2–73.7, 15.1–19.5, 2.1–12.2, and 1.1–1.9%, as analyzed through XPS and elemental analysis (Table S1, Supporting Information). This is plausible because chromium-complexed collagen is predominantly composed of C, O, N, and H and stabilized (tanned) with basic chromium sulfate. The core level C(1s), O(1s), N(1s), and Cr(2p) spectra of core-shell nanostructures derived from chrome shaving waste at different temperatures for 8 h are shown in Figure 2.

The C(1s) core level spectra show a predominant peak around 284 eV corresponding to $\text{C}=\text{C}/\text{C}-\text{C}$ bonds of sp^2 graphitic carbon in aromatic rings when deconvoluted (Figure 2a).¹⁴ A small tail observed in the C(1s) spectra of all the samples can be assigned to $\text{C}-\text{OH}/\text{C}-\text{O}-\text{C}=\text{O}/\text{C}-\text{N}$ functional groups after deconvolution.^{15,16} The O(1s) core level spectra (Figure 2b) exhibit a strong and sharp peak around 531 eV and a weak and broad peak around 535 eV, corresponding to $\text{C}=\text{O}$ and $\text{O}=\text{C}-\text{OH}$, groups, for samples derived from high-temperature treatments (≥ 750 °C).^{14,17} However, low-temperature treatment (500 °C) of chrome shaving waste results in an intense and sharp peak at 530.5 eV, which is assigned to the oxygen present in Cr_2O_3 .¹⁸ This confirms the formation of Cr_2O_3 at low temperature and its conversion to chromium-based nanoparticles at higher temperature, as also seen in the XRD results. Deconvolution of core level N(1s) spectra (Figure 2c) of the core-shell nanostructures exhibit a major peak at 398 eV, which is gradually shifting to 399 eV and then to 401 eV as the temperature of treatment of chrome shaving waste is increased from 500 to 750 °C and then to 1000 °C. The lower energy contributions (398 and 399 eV) are attributed to pyridine-like nitrogen atoms on the edge of a graphene lattice only bonded to two C atoms, and the higher energy peak at 401 eV is assigned to highly coordinated N atoms substituting for inner C atoms (quaternary N) on the graphene layers and bonded to three C atoms.^{19–21} The intensity of the N(1s) peaks is very small compared to C(1s) and O(1s) peaks, indicating that only a minor amount of N is present in these core-shell nanostructures, especially for those obtained from higher temperature treatments (≥ 750 °C). As shown, the relative intensities of the band decrease as the

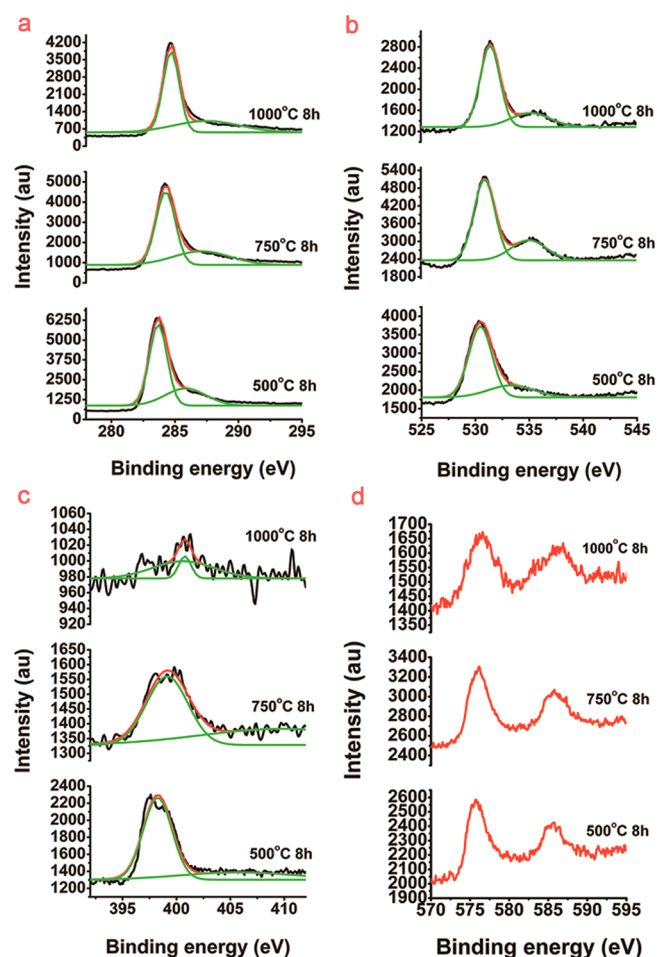


Figure 2. XPS spectra of select Cr-carbon core-shell materials derived from heat treatment of chrome shaving waste at different temperatures for 8 h. (a) High resolution C(1s) core level spectra of Cr-carbon core-shell materials derived from heat treatment of chrome shaving waste at different temperatures for 8 h. (b) High resolution O(1s) core level spectra of Cr-carbon core-shell materials derived from heat treatment of chrome shaving waste at different temperatures for 8 h. (c) High resolution N(1s) core level spectra of Cr-carbon core-shell materials derived from heat treatment of chrome shaving waste at different temperatures for 8 h. (d) High resolution Cr(2p) core level spectra of Cr-carbon core-shell materials derived from heat treatment of chrome shaving waste at different temperatures for 8 h. All the core level spectra were deconvoluted into Gaussian shapes.

temperature increases, which could be due to the conversion of certain nitrogen functionalities into nitrogen gas (N_2) in anoxic conditions at high temperature.²² Thus, it can be seen that the graphitic nanocarbon shells in the Cr-carbons obtained in this study are doped with N and O with varying chemical functionalities as a function of temperature (Figure S1, Supporting Information for further evidence through FT-IR analysis). The core level Cr(2p) spectra of the core-shell nanostructures (Figure 2d) show two major peaks around 576 and 586 eV corresponding to the $2p_{3/2}$ and $2p_{1/2}$ orbital of trivalent chromium. The absence of higher binding energies (579 and 589 eV) confirm the absence of Cr(VI), a carcinogen, when the chrome shaving waste was heated in anoxic conditions²³ (see Figure S2, Supporting Information, for further evidence through EPR analysis). Hence, it is possible that the Cr(III)-collagen matrix is converted into a core-shell

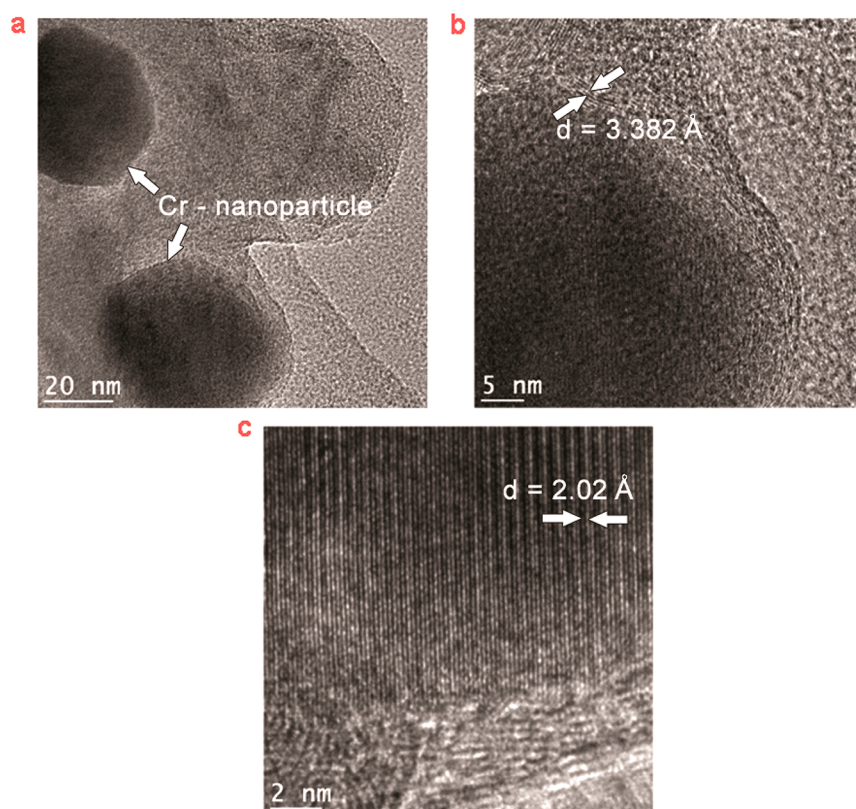


Figure 3. HRTEM images of the Cr-carbon core-shell material derived from chrome shaving waste by treating at 1000 °C for 8 h. (a) Chromium nanoparticles embedded in the carbon shell with an average particle size of ~ 43 nm. (b) Graphitized layers with significant defects surrounding the chromium nanoparticles with an estimated interlayer spacing of 3.382 Å. (c) Chromium nanoparticles showing lattice fringes with an estimated interatomic spacing of 2.02 Å reflecting the (210) plane.

structure with a Cr-based nanoparticle core and a doped graphitic carbon shell.

High Resolution-Transmission Electron Microscopy. HRTEM images of the Cr-carbon core-shell nanostructures synthesized from chrome shaving waste at 1000 °C for 8 h are shown in Figure 3. It is shown that the Cr-based nanoparticles are embedded in the carbon shell (Figure 3a) with an average particle size of ~ 43 nm (see Figure S3, Supporting Information, for further evidence through SEM and particle size distribution analysis). This is in agreement with the values calculated from the XRD data using Scherrer's equation. The carbon shells surrounding the Cr nanoparticles seem to be graphitized with an estimated interlayer spacing of 3.382 Å (Figure 3b). The interplanar d spacing between two graphitic layers in an ideal graphitic structure is 3.354 Å.²⁴ The increase in the interlayer distance could be due to the structural as well as ordering defects owing to the self-doping of nitrogen and oxygen atoms,²⁵ as also shown in our earlier report.⁷ Atomic resolution image shows clear lattice fringes with an estimated interatomic spacing of 2.02 Å that reflects the (210) plane of the Cr-based nanoparticles (Figure 3c). It is possible that the Cr atom can coordinate with the available oxygen ligands at 1000 °C and form a chain of Cr-O bonds longitudinally and align laterally to form Cr-based nanoparticles. The (Cr^{III}-O) bond length in Cr₂O₃ is 1.99 Å,²⁶ which is in good agreement with the observed interatomic distance (2.02 Å). These results confirm the formation of core-shell Cr-nanocarbon materials from chrome shaving waste upon simple heat treatment at 1000 °C in inert atmosphere.

Electrical, Magnetic, and Luminescence Properties.

We have seen that the synthesized core-shell Cr-carbon materials possess significant structural and ordering defects due to the self-doping of N and O atoms, which are expected to contribute significant functional properties such as electrical conductivity, magnetism, and luminescence. Hence, the as-synthesized core-shell Cr-carbon materials were analyzed for electrical conductivity using a standard two-probe method, and the results are shown in Figure 4a. It is seen that the bulk conductivity is increasing for the core-shell materials as a function of treatment temperature and time. The conductivity increases by 6 orders of magnitude when the temperature increased from 500 to 1000 °C, as also evidenced in our earlier study on the synthesis of carbon nano-onions from pristine collagen waste.⁷ The highest conductivity value of $2.2 \times 10^{-1} \text{ S m}^{-1}$ was obtained for the core-shell Cr-carbon material derived from heating chrome shaving waste at 1000 °C for 8 h. This is comparable to the bulk conductivity values reported for pristine graphene powder or sheets.^{27,28} However, these values are much lower than that of pristine graphite or core-shell materials containing conducting polymers or metals or carbon nanotubes reported earlier.^{29,30} The magnetic property of the as-synthesized core-shell Cr-carbon material derived by the heat treatment of chrome shaving waste at 1000 °C for 8 h was analyzed using a VSM at room temperature (Figure 4b). The starting material (chrome shaving waste) has a paramagnetic behavior due to the presence of chromium(III) species bound with collagen (Figure S4, Supporting Information). When it was heated at 1000 °C for 8 h, the formed core-shell Cr-carbon material exhibits a ferromagnetic behavior with

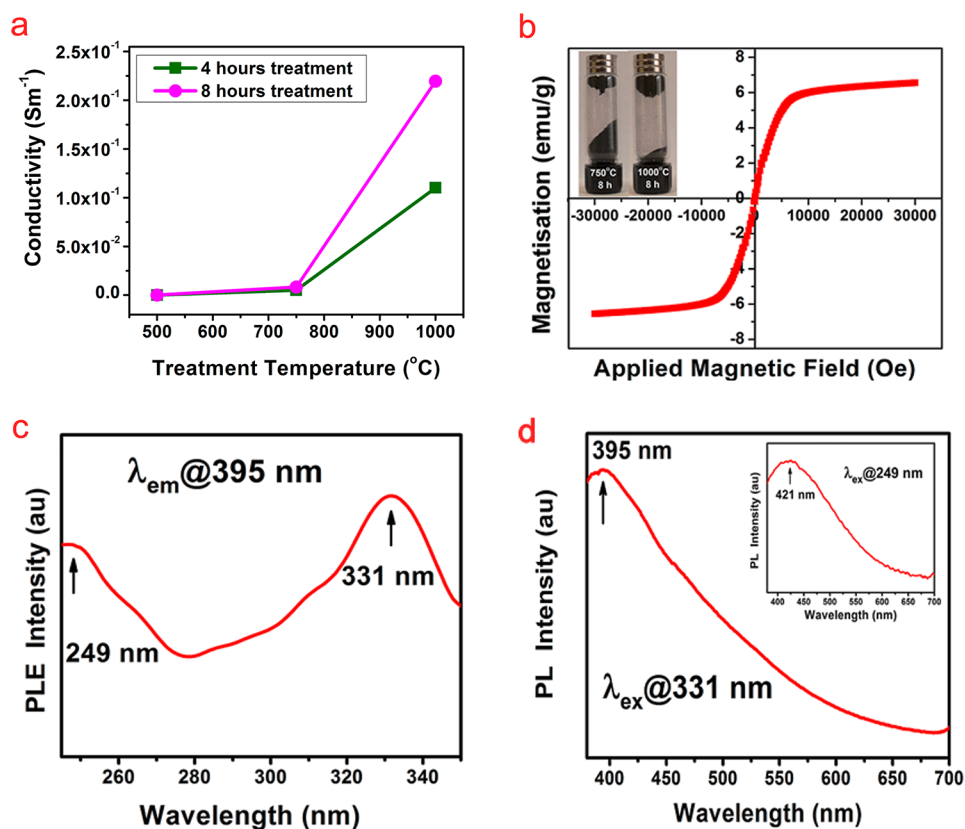


Figure 4. Characterization of the Cr-carbon core-shell materials derived from chrome shaving waste for functional properties. (a) Electrical conductivity of the Cr-carbon core-shell materials as a function of treatment temperature measured by a two-probe method after pressing them into a disc. (b) Room temperature $M(H)$ curve of Cr-carbon core-shell material derived from chrome shaving waste (1000 °C for 8 h) probed using a vibrating sample magnetometer, where the inset shows that more of the Cr-carbon samples (derived by heat treatment of chrome shaving waste at 1000 °C for 8 h) are trapped on the top of the glass vial against the force of gravity under permanent magnets (~ 1000 Oe) compared to the sample obtained at 750 °C for 8 h. (c) Photoluminescence excitation (PLE) spectrum of Cr-carbon derived from high-temperature treatment (1000 °C for 8 h) of chrome shaving waste showing excitations at 249 and 331 nm. (d) Photoluminescence (PL) spectrum of Cr-carbon derived from high-temperature treatment (1000 °C for 8 h) of chrome shaving waste showing emission at 395 nm (excitation at 331 nm), where the inset shows the PL spectrum at 249 nm excitation with emission at 421 nm.

saturation magnetization and high magnetic moment of ~ 6 emu/g, as shown in Figure 4b. This value is slightly higher than the magnetic moment observed for carbon nano-onions synthesized from pristine collagen waste at similar heat treatment conditions.⁷ This may be due to the presence of Cr-based nanoparticles in the core of the derived Cr-carbon core-shell material (see Figure S2, Supporting Information, for further evidence through EPR analysis). Nevertheless, the presence of traces of ferromagnetic impurities, which may arise during processing, cannot be ignored, as shown in our earlier report.⁷ Conversely, our core-shell Cr-carbon nanoparticles still exhibit negligible coercivity and zero remanence, indicating the particles are below their superparamagnetic critical regime, unlike the carbon nano-onions synthesized from pristine collagen waste under similar conditions.⁷ Figure 4c shows the steady state PLE spectra of Cr-carbon core-shell material, derived from heating chromium-collagen waste at 1000 °C for 8 h, recorded at room temperature. It is seen that the main excitation peaks are indexed at 249 and 331 nm. The excitation peak at 249 nm is primarily due to the delocalized π electrons of carbon shells in the excited state and their relaxation to ground state. Here, the other excitation peak at 331 nm is due to the presence of N and O as luminescence centers in the carbon shells of Cr-carbon core-shell material derived from chrome shaving waste fibers. The origin of luminescence here

can be related to our earlier study on carbon nano-onions synthesized from pristine collagen waste under similar conditions.⁷ Here, the role of Cr in the observed luminescence may be insignificant because Cr nanoparticles are surrounded by carbon shells in our synthesized core-shell material. The corresponding steady state (PL) emission spectra of the Cr-carbon core-shell material peaking at 421 and 395 nm are shown in Figure 4d. It should be noted that the emission peak intensity at 331 nm excitation is higher compared to the intensity at 249 nm excitation (see inset of Figure 4d) because the distribution of N and O impurity centers are uniform throughout the carbon shell structure.

Application Studies of Chromium-Encapsulated Graphitic Carbon. As can be seen from the results, the Cr-carbon core-shell nanomaterials synthesized from chrome shaving waste possess significant functionalities such as electrical conductivity, magnetism, and luminescence. Hence, one would expect that these materials could be potentially used in several applications. Indeed, we have recently shown that nanocarbon materials synthesized from pristine collagen waste can be used as the anode for Li-ion battery applications.⁷ Here, we have looked at two applications, namely, (EMI) shielding and catalysis, rather than battery application because it has already been shown that both Cr_2O_3 as well as carbon- Cr_2O_3 composite materials are excellent candidates for Li-ion battery

applications.^{31,32} Highly conducting materials such as carbon nanotubes have been primarily probed for EMI shielding applications.^{33,34} However, electromagnetic waves of both electrical and magnetic fields are at right angle to each other. Hence, it is logical to use a bifunctional material with conducting and magnetic properties. Few attempts were made to introduce magnetic materials such as ferrite or crystalline Fe along with conducting materials to prepare composites in order to enhance the EMI shielding effectiveness.^{35,36} In view of the fact that our autonomously synthesized Cr–carbon core–shell material (1000 °C for 8 h) is both conducting and magnetic, we have studied its use in EMI shielding application after making a pellet with a non-conducting and diamagnetic polyvinyl chloride binder. Figure 5

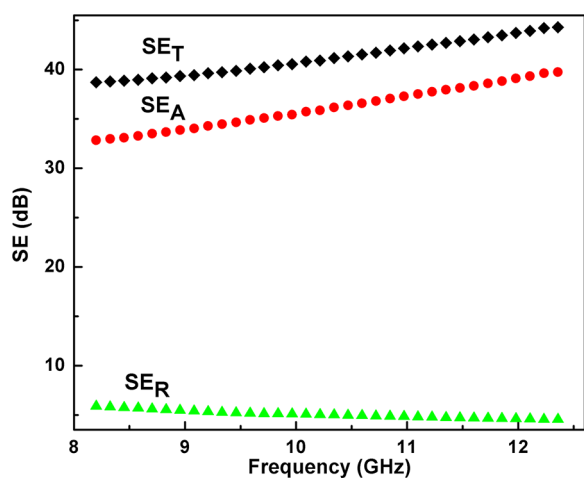


Figure 5. Variation in EMI shielding effectiveness as a function of frequency for the Cr–carbon core–shell material derived from chrome shaving waste (1000 °C for 8 h).

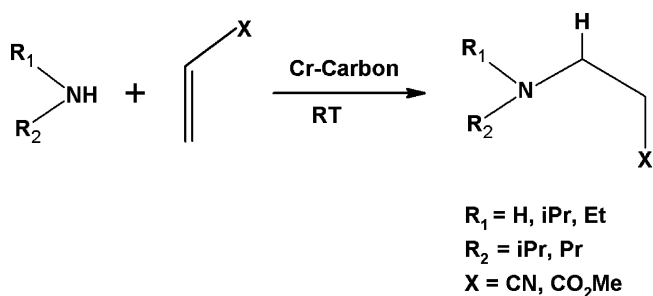
shows the variation of the shielding effectiveness (SE) with frequency in the range of 8.2–12.4 GHz (X-band). When electromagnetic radiation was incident on a slab of shielding material, phenomena such as absorption, reflection, and transmission could be observed. Hence, the total EMI shielding effectiveness (SE_T) is the sum of contributions from absorption (SE_A), reflection (SE_R), and transmission or multiple reflection (SE_M), which can be simply quoted as SE_T (dB) = SE_A + SE_R + SE_M . When $SE_T > 15$ dB for a single layer of shielding material, then SE_M can be neglected ($SE_T \approx SE_A + SE_R$).³³

Here, for our Cr–carbon core–shell material, the shielding effectiveness due to absorption (SE_A) is found to vary from 32.83 to 39.76 dB, while the SE_R varies from 5.88 to 4.54 dB. Thus, the highest SE_T achieved for the Cr–carbon core–shell material is 44.3 dB at 12.4 GHz. Commercial application of EMI shielding material requires a SE value of around 20 dB.³³ Hence, our Cr–carbon core–shell material derived from chromium–collagen waste can be used for a commercial EMI shielding application with appropriate loadings. It is shown that the SE_T is mainly dominated by absorption, while the contribution due to reflection (SE_R) is significantly low. The primary mechanism of EMI shielding is usually a reflection of the electromagnetic radiation incident on the shield, which is a consequence of the interaction of the EMI radiation with the free electrons on the surface of the shielding material.³⁷ Absorption is usually a secondary mechanism of EMI shielding, whereby electric or magnetic dipoles in the shield material

interact with the electromagnetic waves. Shielding by reflection decreases and shielding by absorption increases for higher magnetic permeability shielding material, which provide a magnetic dipole.³⁸ EMI shielding using highly conducting materials such as carbon nanotubes is majorly due to reflection rather than absorption.^{33,34} On the other hand, hybrid magnetic and conducting composite materials provide EMI shielding predominantly due to absorption, owing to the presence of both electric and magnetic dipoles.^{35,39} Analogously, we observed a similar phenomenon for our Cr–carbon core–shell material due to its intrinsic conducting and magnetic properties.

Carbon materials and other heterogeneous carbon-supported metals have been widely used as promising catalysts for extensive range of organic reactions.^{40,41} On the other hand, Cr(III) compounds including Cr_2O_3 are known to catalyze several organic reactions, in particular, oxidation.⁴² In order to assess the catalytic activity of our Cr–carbon core–shell material, we have carried out aza-Michael addition reaction as represented in Scheme 1. The aza-Michael addition reaction is

Scheme 1. Aza-Michael Addition Reaction Catalyzed by Cr–carbon Core-Shell Material



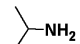
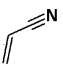
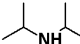
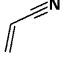
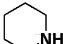
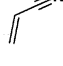
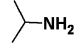
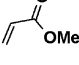
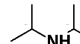
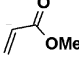
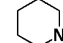
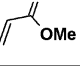
an industrially important transformation in organic chemistry as the products; β -amino compounds, are extensively used in the synthesis of biologically active natural products, antibiotics, antifoam agents, and chiral auxiliaries. However, this direct addition of amines to an electron-rich olefin suffers from a high activation barrier and negative reaction entropy in the absence of a catalyst. Hence, transition metal-catalyzed hydroamination of alkenes is becoming popular,⁴³ although several other catalytic systems are widely experimented. The catalyst is expected to activate the olefin through Lewis acid coordination for nucleophilic attack of the amine. Here, our Cr–carbon core–shell material can catalyze effectively due to the presence of the Cr(III) core and self-doped carbon shells. It is shown from Table 1 that the reaction between the amine and the Michael acceptor without using Cr–carbon as a catalyst was slower with low yield. The presence of catalytic Cr–carbon core–shell material enables the reaction to complete quickly with higher yield.

This trend seems to be the same for all the reactions carried out between different amines and α,β -unsaturated compounds. We believe that the presence of a Cr(III) nanoparticle within the carbon shells containing electron withdrawing groups such as O and N functionalities is responsible for the activation of this industrially important reaction.

CONCLUSIONS

Here, we have shown that Cr–carbon core–shell nanomaterials with rich functionalities can be spontaneously synthesized from

Table 1. Reaction Time and Yield for Aza-Michael Addition of Aliphatic Amines to α,β -Unsaturated Compounds Using Cr–Carbon Core–Shell Material (1000 °C for 8 h) as Catalyst

Entry	Amine	Michael acceptor	Reaction Time (mins)		Yield (%)	
			Without Catalyst	With Catalyst	Without Catalyst	With Catalyst
1			20	7	85	94
2			45	22	45	75
3			15	5	75	95
4			20	10	70	80
5			50	7	75	87
6			45	10	70	85

leather waste by a simple efficient method. The obtained core–shell materials are made up of chromium(III) nanoparticles shielded by graphitic layers with significant self-doping. This new core–shell material is found to be multifunctional due to immense electrical conductivity, luminescence, and room temperature ferromagnetism. We have also shown that it can be potentially used for catalysis as well as EMI shielding applications among various other possible areas. Hence, we demonstrate that leather waste can be instantaneously transformed into high-value Cr–carbon core–shell nanomaterials through a green, simple, scalable, and sustainable approach, which has great potential for various applications.

■ ASSOCIATED CONTENT

📄 Supporting Information

FTIR, EPR, SEM, and atomic composition of the derived Cr–carbon and the VSM analysis of chromium complexed collagen waste. This material is available free of charge via the Internet at <http://pubs.acs.org>.

■ AUTHOR INFORMATION

Corresponding Author

*Tel/Fax: +91 44 24910953. E-mail address: thanik8@yahoo.com.

Notes

The authors declare no competing financial interest.

■ ACKNOWLEDGMENTS

P.T. and M.A. thank CSIR, India, for providing financial support under YSA and ZERIS project schemes. P.T. thanks USIEF, India, for the Fulbright–Nehru Senior Research Fellowship, and B.K.G. thanks IUSSTF, India, for the Indo–US Research Fellowship that enabled their stay at Rice University, Houston, Texas.

■ REFERENCES

- (1) Ajayan, P. M. Nanotubes from carbon. *Chem. Rev.* **1999**, *99*, 1787–1800.
- (2) Allen, M. J.; Tung, V. C.; Kaner, R. B. Honeycomb carbon: A review of graphene. *Chem. Rev.* **2010**, *110*, 132–145.
- (3) Xiong, Y.; Mayers, B. T.; Xia, Y. Some recent developments in the chemical synthesis of inorganic nanotubes. *Chem. Commun.* **2005**, *40*, 5013–5022.
- (4) Ghicov, A.; Albu, S. P.; Macak, J. M.; Schmuki, P. High-contrast electrochromic switching using transparent lift-off layers of self-organized TiO₂ nanotubes. *Small* **2008**, *4*, 1063–1066.
- (5) Wang, Y.; Wang, Y.; Hosono, Wang, K.; Zhou, H. The design of a LiFePO₄/carbon nanocomposite with a core–shell structure and its synthesis by an in situ polymerization restriction method. *Angew. Chem., Int. Ed.* **2008**, *47*, 7461–7465.
- (6) Kim, H.; Cho, J. Superior lithium electroactive mesoporous Si@Carbon core–shell nanowires for lithium battery anode material. *Nano Lett.* **2008**, *8*, 3688–3691.
- (7) Ashokkumar, M.; Narayanan, T. N.; Reddy, A. L. M.; Gupta, B. K.; Chandrasekaran, B.; Talapatra, S.; Ajayan, P. M.; Thanikaivelan, P. Transforming collagen wastes into doped nanocarbons for sustainable energy applications. *Green Chem.* **2012**, *14*, 1689–1695.
- (8) Thanikaivelan, P.; Thiruvilan, A. M.; Chandrasekaran, B.; Rao, J. R.; Nair, B. U. PCT PatentWO2009016649, 2009.
- (9) Rao, J. R.; Thanikaivelan, P.; Sreeram, K. J.; Nair, B. U. Green route for the utilization of chrome shavings (chromium-containing solid waste) in tanning industry. *Environ. Sci. Technol.* **2002**, *36*, 1372–1376.
- (10) Calizo, I.; Balandin, A. A.; Bao, W.; Miao, F.; Lau, C. N. Temperature dependence of the Raman spectra of graphene and graphene multilayers. *Nano Lett.* **2007**, *7*, 2645–2649.
- (11) Warren, B. E. *X-ray Diffraction*; Constable and Company: U.K., 1990; Chapter 13.
- (12) Sharafi, S.; Farhang, M. R. Effect of aluminizing on surface microstructure of an HH309 stainless steel. *Surf. Coat. Technol.* **2006**, *200*, 5048–5051.
- (13) Xing, T.; Cui, X.; Chen, W.; Yang, R. Synthesis of porous chromium carbides by carburization. *Mater. Chem. Phys.* **2011**, *128*, 181–186.
- (14) Akhavan, O. The effect of heat treatment on formation of graphene thin films from graphene oxide nanosheets. *Carbon* **2010**, *48*, 509–519.
- (15) Vinu, A.; Ariga, K.; Mori, T.; Nakanishi, T.; Hishita, S.; Goldberg, D.; Bando, Y. Preparation and characterization of well-ordered hexagonal mesoporous carbon nitride. *Adv. Mater.* **2005**, *17*, 1648–1652.

- (16) Park, S.; An, J.; Jung, I.; Piner, R. D.; An, S. J.; Li, X.; Velamakanni, A.; Ruoff, R. S. Colloidal suspensions of highly reduced graphene oxide in a wide variety of organic solvents. *Nano Lett.* **2009**, *9*, 1593.
- (17) Lakshminarayanan, P. V.; Toghiani, H.; Pittman, C. U. Nitric acid oxidation of vapor grown carbon nanofibers. *Carbon* **2004**, *42*, 2433.
- (18) Shuttleworth, D. Preparation of metal-polymer dispersions by plasma techniques. An ESCA investigation. *J. Phys. Chem.* **1980**, *84*, 1629–34.
- (19) Li, X.; Wang, H.; Robinson, J. T.; Sanchez, H.; Diankov, G.; Dai, H. Simultaneous nitrogen doping and reduction of graphene oxide. *J. Am. Chem. Soc.* **2009**, *131*, 15939–15944.
- (20) Lei, Z.; An, L.; Dang, L.; Zhao, M.; Shi, J.; Bai, S.; Cao, Y. Highly dispersed platinum supported on nitrogen-containing ordered mesoporous carbon for methanol electrochemical oxidation. *Micro-porous Mesoporous Mater.* **2009**, *119*, 30–38.
- (21) Casanovas, J.; Ricart, J. M.; Rubio, J.; Illas, F.; Mateos, J. M. J. Origin of the large N 1s binding energy in X-ray photoelectron spectra of calcined carbonaceous materials. *J. Am. Chem. Soc.* **1996**, *118*, 8071–8076.
- (22) Wu, Z.; Sugimoto, Y.; Kawashima, H. Formation of N₂ from pyrrolic and pyridinic nitrogen during pyrolysis of nitrogen-containing model coals. *Energy Fuels* **2003**, *17*, 694–698.
- (23) Park, D.; Yun, Y. S.; Park, J. M. XAS and XPS studies on chromium-binding groups of biomaterial during Cr(VI) biosorption. *J. Colloid Interface Sci.* **2008**, *317*, 54–61.
- (24) Jones, L. E.; Thrower, P. A. Influence of boron on carbon fiber microstructure, physical properties, and oxidation behavior. *Carbon* **1991**, *29*, 251–269.
- (25) Chen, X. H.; Deng, F. M.; Wang, J. X.; Yang, H. S.; Wu, G. T.; Zhang, X. B.; Peng, J. C.; Li, W. Z. New method of carbon onion growth by radio-frequency plasma-enhanced chemical vapor deposition. *Chem. Phys. Lett.* **2001**, *336*, 201–204.
- (26) Kim, T. W.; Hur, S. G.; Hwang, S. J.; Park, H.; Choi, W.; Choy, J. H. Heterostructured visible-light-active photocatalyst of chromia-nanoparticle-layered titanate. *Adv. Funct. Mater.* **2007**, *17*, 307–314.
- (27) Choucair, M.; Thordarson, P.; Stride, J. A. Gram-scale production of graphene based on solvothermal synthesis and sonication. *Nature Nanotechnol.* **2009**, *4*, 30–33.
- (28) Li, X.; Zhang, G.; Bai, X.; Sun, X.; Wang, X.; Wang, E.; Dai, H. Highly conducting graphene sheets and Langmuir–Blodgett films. *Nature Nanotechnol.* **2008**, *3*, 538–542.
- (29) Rana, S.; Cho, J. W. Core–shell morphology and characterization of carbon nanotube nanowires click coupled with polypyrrole. *Nanotechnology* **2011**, *22*, 275609.
- (30) Rotzetter, A. C. C.; Luechinger, N. A.; Athanassiou, E. K.; Mohn, D.; Koehler, F. M.; Grass, R. N. Sintering of core–shell Ag/glass nanoparticles: metal percolation at the glass transition temperature yields metal/glass/ceramic composites. *J. Mater. Chem.* **2012**, *20*, 7769–7775.
- (31) Liu, H.; Du, X.; Xing, X.; Wang, G.; Qiao, S. H. Highly ordered mesoporous Cr₂O₃ materials with enhanced performance for gas sensors and lithium ion batteries. *Chem. Commun.* **2012**, *18*, 865–867.
- (32) Guo, B.; Chi, M.; Sun, X. G.; Dai, S. Mesoporous carbon–Cr₂O₃ composite as an anode material for lithium ion batteries. *J. Power Sourc.* **2012**, *205*, 495–499.
- (33) Li, N.; Huang, Y.; Du, F.; He, X.; Lin, X.; Gao, H.; Ma, Y.; Li, F.; Chen, Y.; Eklund, P. C. Electromagnetic interference (EMI) shielding of single-walled carbon nanotube epoxy composites. *Nano Lett.* **2006**, *6*, 1141–1145.
- (34) Yang, Y.; Gupta, M. C. Novel carbon nanotube-polystyrene foam composites for electromagnetic interference shielding. *Nano Lett.* **2005**, *5*, 2131–2134.
- (35) Che, R.; Peng, L. M.; Duan, X.; Chen, Q.; Liang, X. Microwave absorption enhancement and complex permittivity and permeability of Fe encapsulated within carbon nanotubes. *Adv. Mater.* **2004**, *16*, 401–405.
- (36) Yavuz, O.; Ram, M. K.; Aldissi, M.; Poddar, P.; Hariharan, S. Synthesis and the physical properties of MnZn ferrite and NiMnZn ferrite–polyaniline nanocomposite particles. *J. Mater. Chem.* **2005**, *15*, 810–817.
- (37) Chung, D. D. L. Electromagnetic interference shielding effectiveness of carbon materials. *Carbon* **2001**, *39*, 279–285.
- (38) Vovchenko, L.; Matzui, L.; Oliynyk, V.; Launetz, V.; Normand, F. L. Anomalous microwave absorption in multi-walled carbon nanotubes filled with iron. *Physica E* **2012**, *44*, 928–931.
- (39) Singh, A. P.; Mishra, M.; Chandra, A.; Dhawan, S. K. Graphene oxide/ferrofluid/cement composites for electromagnetic interference shielding application. *Nanotechnology* **2011**, *22*, 465701–465709.
- (40) Zhao, J.; Cheng, F.; Yi, C.; Liang, J.; Tao, Z.; Chen, J. Facile synthesis of hierarchically porous carbons and their application as a catalyst support for methanol oxidation. *J. Mater. Chem.* **2009**, *19*, 4108–4116.
- (41) Yoon, H.; Ko, S.; Jang, J. Nitrogen-doped magnetic carbon nanoparticles as catalyst supports for efficient recovery and recycling. *Chem. Commun.* **2007**, *14*, 1468–1470.
- (42) Muzart, J. Chromium-catalyzed oxidations in organic synthesis. *Chem. Rev.* **1992**, *92*, 113–140.
- (43) Hultzsck, K. C. Transition metal-catalyzed asymmetric hydroamination of alkenes (AHA). *Adv. Synth. Catal.* **2005**, *347*, 367–391.